Semantic Learning for Molecular Communication in Internet of Bio-Nano Things

Hanlin Cai, Ozgur B. Akan
Department of Engineering, University of Cambridge, Cambridge, U.K.
hc663@cam.ac.uk, oba21@cam.ac.uk

***Abstract*—Molecular communication (MC) underpins the Internet of Bio-Nano Things (IoBNT) but suffers from low data rates, noise, and inter-symbol interference (ISI). To address these challenges, this paper proposes an end-to-end semantic learning framework that prioritizes task-relevant information for biomedical diagnostics under resource constraints. A deep encoder–decoder architecture extracts and quantizes semantic features, while a probabilistic channel network models molecular propagation, enabling gradient-based optimization. Experimental results demonstrate that the proposed semantic framework improves diagnostic accuracy by at least 25% compared to conventional JPEG compression with LDPC coding methods under resource-constrained molecular communication scenarios.**

I. Introduction

Molecular communication (MC) has emerged as a promising mechanism for information exchange in environments where electromagnetic (EM)-based systems face fundamental constraints. By relying on the controlled release, propagation, and detection of molecules, MC suits Internet of Bio-Nano Things (IoBNT) applications such as disease diagnosis, targeted drug delivery, and real-time health monitoring [1]. Despite its potential, practical MC deployment encounters serious challenges including low data rates, severe inter-symbol interference (ISI), and high susceptibility to noise, making it difficult to support complex transmissions under the stochastic nature of molecular propagation [2]. To address these issues, recent efforts have integrated semantic communication into MC, prioritizing task-relevant information over traditional bit-level transmission [3], [4]. While such approaches have shown promise, they often lack a structured mapping between high-level features and the physical constraints of molecular channels. In this paper, we propose an end-to-end semantic MC framework using a deep encoder-decoder architecture to extract, quantize, and decode task-specific features. We introduce a quantization function to refine the semantic-to-physical mapping and employ a probabilistic channel network to model MC's stochastic propagation, enabling end-to-end differentiability and adaptation. This strategy prioritizes task-specific semantic content, offering enhanced efficiency and robustness in biomedical diagnostic classification scenarios.

II. System Model

This work consider a SISO system in an unbounded 3D environment with constant flow velocity v. At the beginning of each symbol slot of duration t_s, the transmitter (Tx) releases up to n_m molecules, which diffuse with coefficient D_c and drift along v. For large n_m, the number of molecules arriving at the receiver (Rx) by time t can be approximated by

$$N(n_m, t) \sim \mathcal{N}\Big(n_m P(t),\, n_m P(t)\big[1 - P(t)\big]\Big), \quad (1)$$

where $P(t)$ is single-molecule arrival probability [5]. Residual molecules from earlier slots lead to inter-symbol interference (ISI), and additive Gaussian noise $N_{\text{noise}} \sim \mathcal{N}(0, \sigma_n^2)$ further degrades detection. To quantify system performance, we define the signal-to-interference ratio (SIR) of the j-th symbol as

$$SIR = \frac{W[j]\, N(n_m, t)}{\sum_{i=1}^{\lambda} W[j-i]\, N\big(n_m,\, t + i\, t_s\big) \;+\; N_{\text{noise}}}, \quad (2)$$

where $W[j] \in [0, 1]$ represents the fraction of n_m released in the j-th slot, and λ is the channel memory capturing ISI effects. As illustrated in Fig. 1, we employ a deep encoder-decoder framework for task-specific semantic transmission. The encoder extracts a low-dimensional feature vector from input data (e.g., biomedical images) and performs probabilistic quantization to produce normalized channel symbols W. Concretely, the encoder first generates a semantic feature $\mathcal{F} = f_\theta(\chi)$, which is then mapped to W via a neural network $Q_\beta(\cdot)$, ensuring $W_i \in [0, 1]$. At the receiver, the decoder $g_\psi(\cdot)$ infers task-specific outputs (e.g., classification results) from the received symbols W_{Rx}. To capture the stochastic behavior of the MC channel, we introduce a probabilistic channel network that models $p(W_{\text{Rx}}|W) = \sum_{i=1}^{h} \pi_i(W)\varphi_i(W_{\text{Rx}}|W)$, where $\pi_i(\cdot)$ are mixing coefficients, and the Gaussian kernel is [6]:

$$\varphi_i\big(W_{\text{Rx}} \mid W\big) = \frac{1}{\sqrt{2\pi\, \sigma_i^2(W)}} \exp\Big[-\tfrac{\|W_{\text{Rx}} - \mu_i(W)\|^2}{2\, \sigma_i^2(W)}\Big], \quad (3)$$

where $\mu_i(W)$ and $\sigma_i^2(W)$ are learned parameters, enabling a differentiable approximation of diffusion, drift, ISI, and noise effects. This channel network is trained independently to estimate $p(W_{\text{Rx}}|W)$, then integrated into the end-to-end encoder decoder framework to support gradient-based optimization of semantic transmission under resource-constrained scenarios.

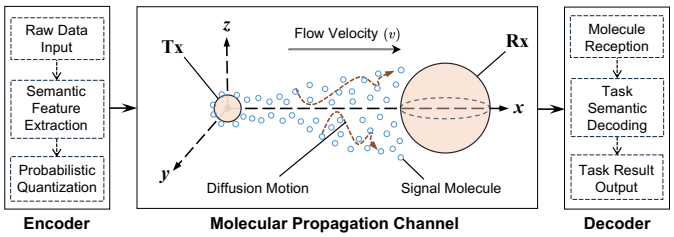

Fig. 1. Illustration of the semantic molecular communication framework.

TABLE I
PARAMETERS OF THE MOLECULAR PROPAGATION CHANNEL

Parameter	Scenario 1	Scenario 2
Propagation distance (R)	$100\,\mu$m	60 cm
Receiver radius (r)	$20\,\mu$m	$20\,\mu$m
Flow velocity (v)	$50\,\mu$m/s	40 cm/s
Symbol duration (t_s)	4 s	3 s
Diffusion coefficient (D_c)	$800\,\mu\text{m}^2/\text{s}$	$800\,\mu\text{m}^2/\text{s}$
Maximum released molecules (n_m)	2×10^4	2×10^4

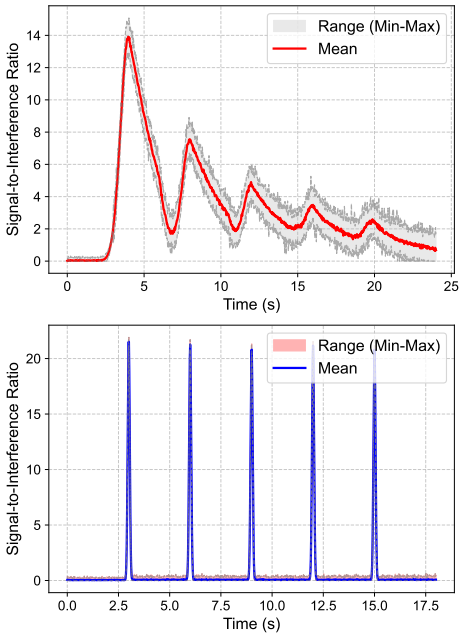

Fig. 2. Temporal variations of SIR during the transmission of a continuous sequence of five '1' symbol bits in two molecular communication scenarios.

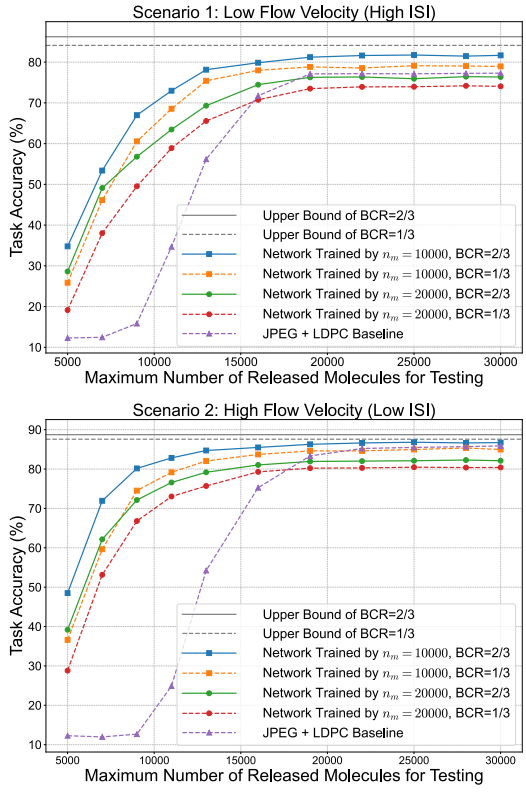

Fig. 3. Accuracy performance comparison between different methods in two molecular communication scenarios (BCR: Bandwidth Compression Ratio).

III. EXPERIMENT AND EVALUATION

The proposed framework is evaluated using the Kvasir dataset [7], which contains 8,000 high-resolution gastrointestinal images covering eight clinically significant categories, including normal findings and pathological conditions (e.g., polyps, ulcers, and bleeding). Each image is resized to 128×128 pixels with RGB channels preserved to retain critical diagnostic features. As summarized in Table I, two distinct communication scenarios with different propagation distances, flow velocities, and symbol durations are considered to simulate practical IoBNT environments [5].

Fig. 2 depicts the temporal variations of SIR during the propagation of five consecutive '1' symbol bits via the trained channel network in two communication scenarios. The results indicate that the proposed channel network closely replicates the physical characteristics of molecular propagation by accurately capturing the pronounced ISI at low flow velocity and the accelerated molecular clearance at high flow velocity.

Fig. 3 compares the performance of the proposed semantic framework for diagnostic classification tasks under different parameter settings with the conventional JPEG and LDPC-based approach [8]. The Bandwidth Compression Ratio (BCR) represents the ratio of the compressed feature size to the original input data size, indicating the level of data reduction achieved before transmission. The results show that the proposed method significantly improves accuracy of classification tasks, achieving at least a 25% performance gain over traditional methods in resource constraint condition ($n_m < 12,000$). Notably, networks trained with lower n_m values exhibit better learning efficiency, as the increased impact of ISI and channel degradation enables the model to capture more robust propagation features, effectively mitigating the cliff effect observed at low released molecule levels.

REFERENCES

[1] O. B. Akan, H. Ramezani, T. Khan, N. A. Abbasi, and M. Kuscu, "Fundamentals of molecular information and communication science," *Proceedings of the IEEE*, vol. 105, no. 2, pp. 306–318, 2016.

[2] O. T. Baydas, O. Cetinkaya, and O. B. Akan, "Estimation and detection for molecular mimo communications in the internet of bio-nano things," *IEEE Transactions on Molecular, Biological and Multi-Scale Communications*, vol. 9, no. 1, pp. 106–110, 2023.

[3] J. Zhu, C. Bai, Y. Zhu, X. Lu, and K. Wang, "Evolutionary generative adversarial network based end-to-end learning for mimo molecular communication with drift system," *Nano Communication Networks*, vol. 37, p. 100456, 2023.

[4] C. Yukun, C. Wei, and A. Bo, "Building semantic communication system via molecules: An end-to-end training approach," *China Communications*, vol. 21, no. 7, pp. 113–124, 2024.

[5] V. Jamali, A. Ahmadzadeh, W. Wicke, A. Noel, and R. Schober, "Channel modeling for diffusive molecular communication—a tutorial review," *Proceedings of the IEEE*, vol. 107, no. 7, pp. 1256–1301, 2019.

[6] D. García, J. O. Lacruz, D. Badini, D. De Donno, and J. Widmer, "Model-free machine learning of wireless siso/mimo communications," *Computer Communications*, vol. 181, pp. 192–202, 2022.

[7] P. H. Smedsrud, V. Thambawita, S. A. Hicks, H. Gjestang, O. O. Nedrejord, E. Næss, H. Borgli, D. Jha, T. J. D. Berstad, S. L. Eskeland *et al.*, "Kvasir-capsule, a video capsule endoscopy dataset," *Scientific Data*, vol. 8, no. 1, p. 142, 2021.

[8] W. Yang, H. Du, Z. Q. Liew, W. Y. B. Lim, Z. Xiong, D. Niyato, X. Chi, X. Shen, and C. Miao, "Semantic communications for future internet: Fundamentals, applications, and challenges," *IEEE Communications Surveys & Tutorials*, vol. 25, no. 1, pp. 213–250, 2022.